Design and Comprehensive Analysis of Maximum Power Point Tracking Techniques in Photovoltaic Systems

Ali M. Eltamaly, Mohamed A. Mohamed, and Ahmed G. Abo-Khalil

Abstract In this chapter the performance of various maximum power point tracking techniques for Photovoltaic (PV) systems has been presented, under uniform and non-uniform irradiance conditions. Under uniform irradiance conditions, the power-voltage curve of PV systems is nonlinear and contains one peak point whose location appertains to the irradiation and surface temperature of the PV system. Partial shading on PV modules reduces the generated power than the maximum power generated from each module separately. The traditional techniques of tracking the maximum power point are designed to track the global peak but they always failed to capture the exact point. In this chapter, different techniques of maximum power point tracking have been introduced, analyzed, and simulated. MATLAB, SIMULINK, and PSIM software have been utilized to simulate the PV systems under various shading conditions. Furthermore, the response of the different techniques of maximum power point trackers has been evaluated under different weather conditions.

Keywords Photovoltaic · Maximum power point tracking · Partial shading · PSIM · Optimal design · Solar energy

A. M. Eltamaly (✉)
Electrical Engineering Department, Faculty of Engineering, Mansoura University, Mansoura 35511, Egypt
e-mail: eltamaly@ksu.edu.sa

Sustainable Energy Technologies Center, King Saud University, Riyadh 11421, Saudi Arabia

K.A. CARE Energy Research and Innovation Center, Riyadh 11451, Saudi Arabia

M. A. Mohamed
Electrical Engineering Department, Faculty of Engineering, Minia University, Minia 61519, Egypt
e-mail: dr.mohamed.abdelaziz@mu.edu.eg

A. G. Abo-Khalil
Department of Electrical Engineering, College of Engineering, Majmaah University, Almajmaah 11952, Saudi Arabia
e-mail: a.abokhalil@mu.edu.sa

Department of Electrical Engineering, College of Engineering, Assuit University, Assuit 71515, Egypt

1   Introduction

The solar PV technology is currently progressing and appearing the capability of being utilized in isolated and grid-connected applications [1, 2]. The limitations that have kept the exceptionally expansive scale use of PV so far are the initial high costs requirement and low efficiency [3]. Although, with late advances, the cost is descending by utilizing advanced technology in the manufacture of PV modules [4]. Proficiency is enhancing by utilizing multilayers of PV solar cells [5]. Current research is coordinated on progressing existing modules, for example, the thin-film and new material for crystalline cell technologies [6, 7]. Figure 1 appearing and anticipated capital expense of sun-oriented photovoltaics. Figure 2 demonstrates the world total establishment from 2004 to 2014. Before the finish of 2017, the global-introduced PV capacity hops to 303 GW [8]. Utilizing PV in Hybrid Renewable Energy Systems (HRES) is a decent choice where the sensible cost of the PV system and the great connection between the generation and the load [9]. This will diminish the extent of the storage system utilized in HRES particularly if the ideas of the smart grid are considered [10].

Solar power is converted into electricity by photovoltaic (PV) technology as shown in Fig. 3, or concentrating solar power (CSP) as shown in Fig. 4. The following sections introduce a brief review of these technologies:

A. The Technology of Solar Photovoltaic (PV)

In the late 1880s the photovoltaic technology was discovered but did not gain significance until 1954 when it was rediscovered by Bell Telephone [12]. Fundamentally, the PV technology employs silicon and some other materials device to entrap sunlight known as photons that will hit the free electrons in the silicon device to produce an electric voltage by a process referred to as the photovoltaic effect. This process produces direct current (DC) electricity power. The PV system produced power is a
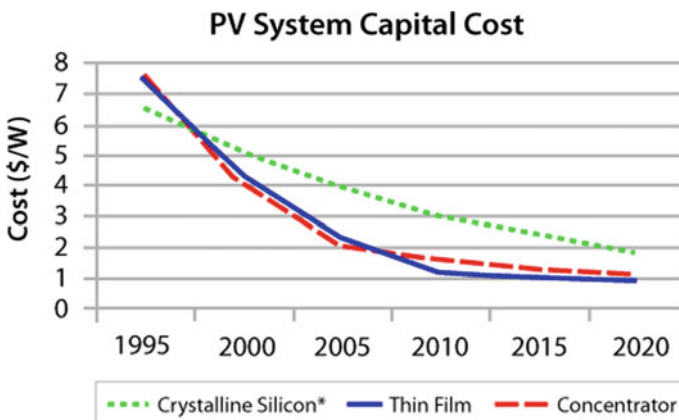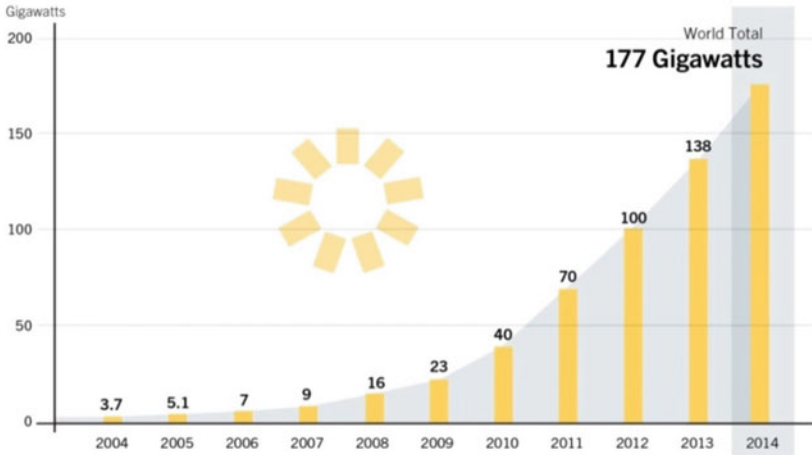

Fig. 1 The historical and projected capital cost of solar photovoltaics [9]

Solar PV Global Capacity, 2004–2014

REN21 *Renewables 2015 Global Status Report*

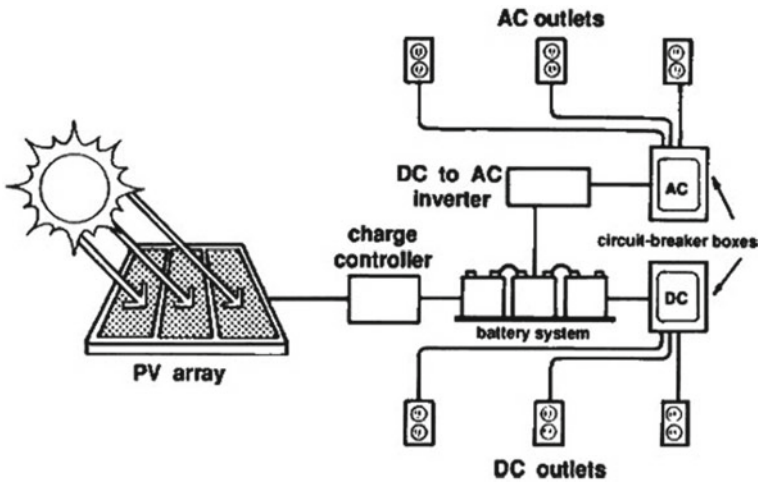**Fig. 2** World cumulative installation from 2004 to 2014 [7]

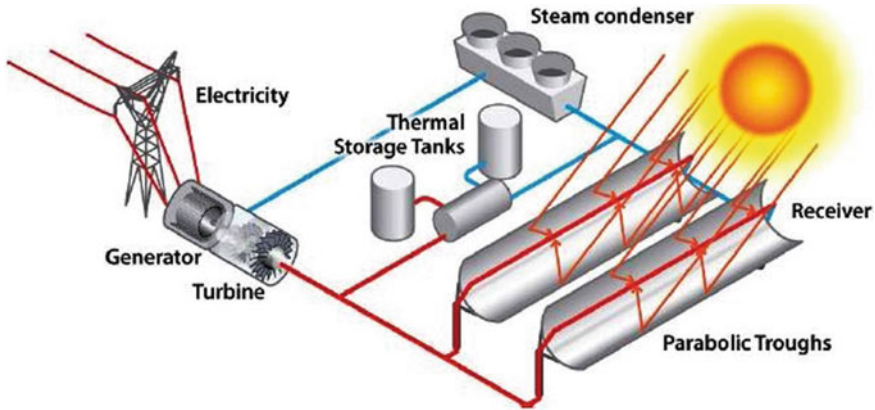**Fig. 3** Photovoltaic energy system [10]

Fig. 4 Concentrated solar power tower plant [11]

function of the output voltage as shown in Fig. 5. The research literature has produced several mathematical models of the PV cell. Some aspects of the literature will be discussed in the chapters to come. Figure 5 shows the output power versus terminal voltage relation under various radiation and temperature. This figure shows that there is a maximum power point (MPP) located for each terminal voltage [13]. This is the reason why there are many variations in MPP trackers (MPPT) as introduced in many research publications [14].

Many types of materials are utilized to design the PV-cells and they are different in their characteristics. The most popularly used PV-cells are the crystalline silicon [15]. PV-cells from crystalline silicon have been in use for a long time and it is now a
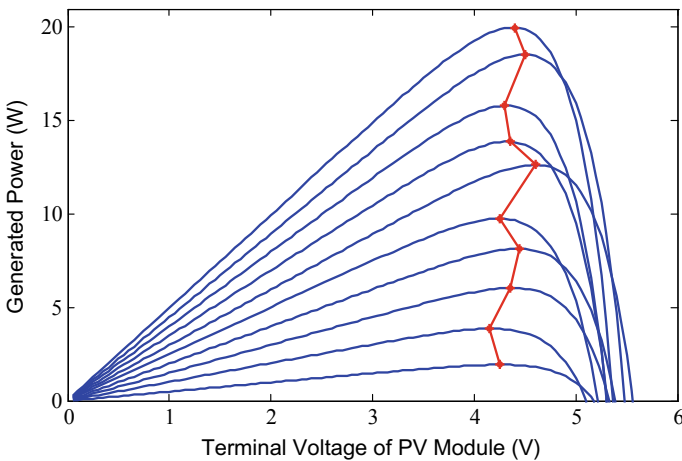

Fig. 5 The output power Versus terminal voltage relation under various radiation and temperature [14]

matured technology in the manufacturing technology with its price becoming lower and lowers especially in the presence of mass-fraction production. As a result, this chapter will concentrate more on the crystalline silicon PV-cells. PV-cells of other types have a similar analysis but with dissimilar performance characteristics [14]. The converter efficiency of PV-cell ranges from 10 to 25% subject to the materials being used in the fabrication of the PV-cells [16]. Besides, PV module's power is determined by PV modules to tilt angle and temperature [17]. The presence of dust can reduce the efficiency of the PV systems and it should be cleaned frequently using different technologies [18].

The PV system' DC-generated power is used to charge a battery or be converted into alternating current (AC) employing power electronics inverter for AC appliances. The PV system can be used as a standalone or part of a hybrid system to support remote loads far away from the electric utility or may be interconnected with the electric utility [19].

In a grid-intertie system, the PV configuration is tied directly to the electric network using DC/AC inverter. If the PV system generates power over its local load requirement, the extra generated power is transferred to the electric utility. If the PV local load has a deficiency in power from the PV system, the load can absorb extra power from the electric utility [20]. The grid-intertie with battery backup is an extended version of the former with the inclusion of battery to store power for periods when the grid is not available.

The isolated or grid-independent solar systems are utilized in decentralized applications and remote areas away from the network [21]. These systems require storage batteries facilities, DC/AC inverters, and charge controllers. The isolated HRES is usually utilized in hybrid systems where diesel generators can be used as an auxiliary when the generated power from HRES is lower than the demand requirements [22]. The following are the configurations used to mount the PV modules:

1. *Flat-Plate Modules*

The PV systems can be used as a flat-plate configuration which requires a large number of cells and larger land areas. The flat plate should face the sun in the best way as possible and there is a compromise between this need with the cost. The best tilt angle for the PV modules is the site's latitude angle. Other systems continuously change the module's tilt angle to a monthly or seasonal best tilt angle. Another alternative is to use a solar tracking system to track the sun using one-axis or two-axis tracking systems but this comes with an increase in cost. Hence, a careful analysis of the compromise between the cost of the tracking system and the increase of energy due to using sun trackers must be analyzed in detail. The different configurations used to mount the PV modules are listed in the following points:

- Fixed tilt angle arrays
- Systems adjusted to the monthly best tilt angle
- Systems adjusted to the seasonally best tilt angle
- One-axis tracking
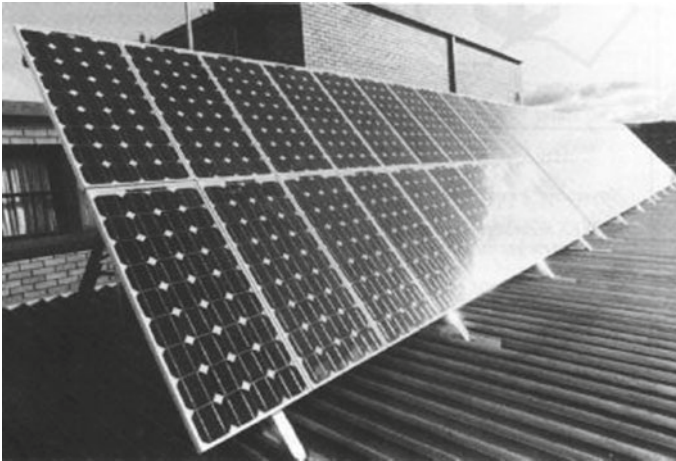
Fig. 6 Fixed tilt angle, FTA photovoltaic system [24]

- Two-axis tracking
- Concentrator arrays

2. *Fixed Tilt Angle Arrays*

In this method, the modules are fixed facing north in the southern hemisphere at a tilt angle comparable to the site's latitude [14, 23]. The best tilt angle approximately equals the latitude of the site facing the equator in the north and south of the earth [24]. Figure 6 shows a Fixed Tilt Angle (FTA) photovoltaic system.

3. *Monthly Adjusted Tilting*

An alternative to using a fixed tilt angle of the photovoltaic array is to vary the tilt monthly depending on the monthly optimum tilt angle. The literature approximate 8% [24] increase in energy captured by the photovoltaic compared to the fixed optimum tilt angle. The optimum tilt angle is either adjusted manually or by using an electromechanical system. Literature concluded that the adjustment to the tilt angles every three months increases the annual energy production by about 5% [25]. This increase may not be economically beneficial, considering the cost of implementation. In monthly adjusted tilted arrays, the monthly best tilt angle can be estimated for the site, and then the array's monthly angle can be adjusted. This method has no complexity and yields increased efficiency. Figure 7 shows Adjustable Tilt Angle, ATA photovoltaic system with monthly adjusted tilting.

4. *One-Axis Tracking*

One-axis tracking is used to actively track the sun during the day time. The tracking is done each hour or in a lower period. This system changes the angle concerning the vertical axis and the tracking starts in the morning where the array faces the

Fig. 7 Adjustable tilt angle, ATA photovoltaic system [25]

east and at the end of the day when it faces the west. Output can be increased considerably concerning the previous techniques. One-axis tracking can increase the energy captured by 20–30% in comparison with the optimum fixed tilt angle [25] as discussed above. A single-axis tracking array, SAST photovoltaic system is shown in Fig. 8. The system installation and maintenance cost could be higher than the increase in energy captured and this is the reason why it is not recommended to use this system in commercial photovoltaic energy systems.

5. *Two-Axis Tracking*

In this configuration, the output energy can be increased higher than the previous techniques. Nearly 30% insolation improvement relative to an optimum fixed tilt array is achievable. However, both the capital and maintenance costs are high hence only a few large systems are presently installed. Also, it needs more space to freely

Fig. 8 SAST concentrator solar cell array [26]

Fig. 9 TAST concentrator solar cell array [25]

move the two-axis systems. The two-axis tracking system, TAST photovoltaic system is shown in Fig. 9. By mounting the array on a two-axis sun tracking, from 30% [24] to 40% [25] more solar energy can be collected over the year than in fixed tilt installation. Furthermore, the gain is mostly in the early morning and late evening, when it is particularly valuable in meeting peak loads.

6. *Concentrator PV Arrays*

The concentrator PV arrays utilize optical lenses or mirrors to focus the solar radiation on high-efficiency PV arrays. Precise tracking of the sun is required for these systems, principally when the concentration ratio is high. Tracking increases the intercepted insolation but with concentrators, the trade-off is the ability to access only the direct fraction. The overall outcome depends on the clarity of the sky at the site. The concentrators will only use the direct beam light; the diffuse light cannot be implemented. To increase total annual energy output the concentrators will require tracking devices. Although the expenses will increase, the increase in annual energy output is up to 30% in comparison to the increase by using just the tracking devices. Another additional advantage of using concentrators is that it uses a reduced number of solar cells and hence the area needed for installation. There are many types of concentrators as mentioned below [27]:

(a) *Parabolic troughs:* Silvered glass and polished aluminized flexible film are used in reflective materials. This type is shown in Fig. 10a.
(b) *The ordinary lens:* Glass lens collects the sunlight in the small solar cell area. This type is shown in Fig. 10b.
(c) *Fresnel lens:* Fresnel lens similarly diffracts the sunrays as would be done by a conventional lens. The advantage of a fresnel lens is that; it is much thinner and lighter than a conventional lens. The fresnel lens and parabolic trough concentrator have received the most attention for use in the photovoltaic system. This type is shown in Fig. 10c.
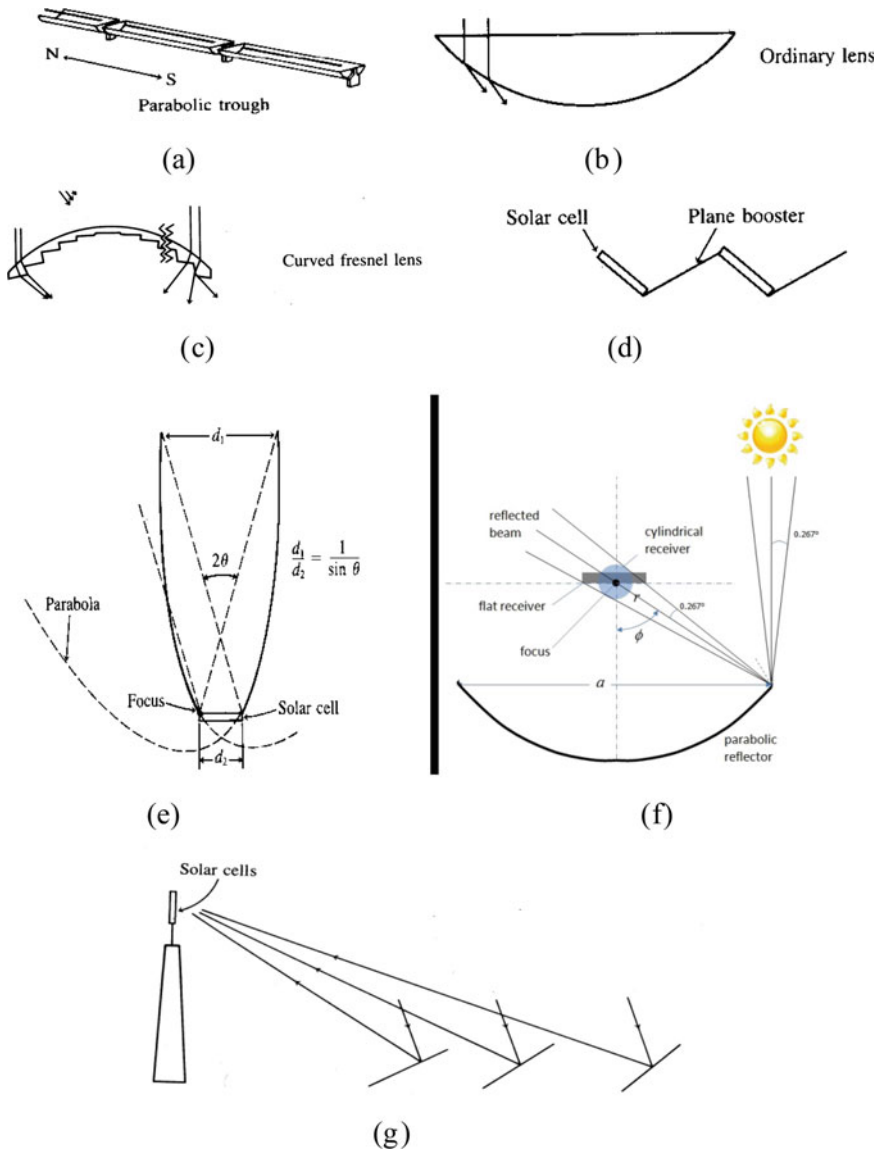
Parabolic trough

(a)

Ordinary lens

(b)

Curved fresnel lens

(c)

Solar cell   Plane booster

(d)

$$\frac{d_1}{d_2} = \frac{1}{\sin \theta}$$

Parabola

Focus

Solar cell

(e)

reflected beam

cylindrical receiver

flat receiver

focus

parabolic reflector

(f)

Solar cells

(g)

Fig. 10 Types of concentrator [27]

(d)   ***Plan booster concentrator:*** This is the simplest form of flat-plate concentrator or booster. The solar cell output can be improved by about 50% [27]. This type of concentrator is proposed to be used with a space-satellite photovoltaic generation station. This type is shown in Fig. 10d.

(e) **Compound parabolic concentrator:** This was proposed by Winston proposes in 1974 [28]. This concentrator referred to as a Winston collector, is formed with two parabolic cups that satisfy two conditions. This type is shown in Fig. 10e.

(f) **Parabolic Dish:** Parabolic dish requires two axes sun tracking system and provides a very high concentration ratio. This type is shown in Fig. 10f.

(g) **Central receiver concentrator: The total mirror surface in one module can collect** from tens of kilowatts to tens of megawatts. The concentrator solar cell systems trade the added costs of the optical concentrator for the cost of solar cells since a concentrator system uses a much smaller quantity of solar cells than flat-plate systems of the same capacity. This type is shown in Fig. 10g.

B. The Technology of Concentrating Solar Power (CSP)

The main types of CSP are power tower systems, linear concentrators, and dish/engine CSP systems. The CSP systems are rarely utilized in isolated hybrid energy systems. Most of the applications of CSP are utility integration systems because it is economically to install it in large central power plants.

Solar energy is becoming more attractive and it is counted as future energy. Solar thermal energy or CSP is the most important option of renewable energies to provide clean electric energy shortly [26].

The operation of CSP plants depends on concentrating the sun's energy by using solar mirrors to increase the heat on a boiler which can be used to produce super steam to hit a blade of a steam turbine to convert heat energy into mechanical energy and then into electric energy using electric generators. Heat storage can store heat in the day time to be converted later to electricity at night or cloudy days. Active researchers have used certain oil; some salts materials, some types of sand as heat storage. The need for heat storage is not an important issue in the utility integration of CSP because of the correlation between most of the loads and the power generated from the sun which makes it preferable to be direct feeds the loads through the electric grid.

Many techniques have been used in the generation of electricity from CSP systems. Four main technologies can be used to generate electric power from solar thermal plants. These techniques are briefly discussed and shown in the following sections:

1. Trough Systems

A trough-shaped mirror is used to reflect the solar radiation in a tube in the focus of mirrors. The pipe in the center of the trough mirror is called "absorber pipe," or "heat collection element." Figure 11 shows the trough system as a part of the solar thermal system. Most of the trough systems use a axis sun tracker system to ensure that the mirrors reflect the sun's rays on the receiver all time.

2. Solar Tower Systems

Solar tower systems also called central receivers in which many flat heliostats (mirrors) are used to reflect the sun rays onto a tower called a receiver as shown
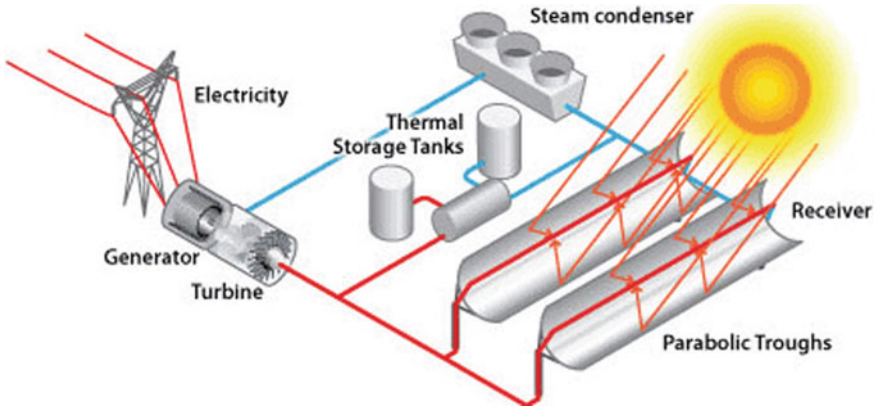
Fig. 11 Trough system [26]

in Fig. 12 [21]. The heliostats rotate with two-axis control systems that can track the sun's movement one axis to capture the sun during the day and the other one is to track it through the year. The mirrors are focusing on the receiver located at top of the tower to heat the fluid, such as molten salt, as hot as 1,050°F. The electricity generation can be achieved by direct use of the hot fluid or the heat can be stored in
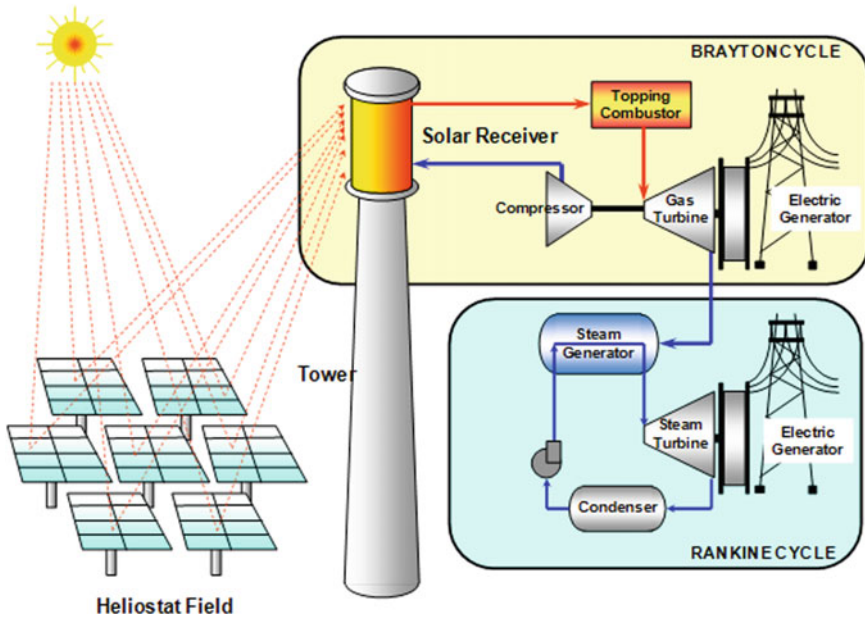
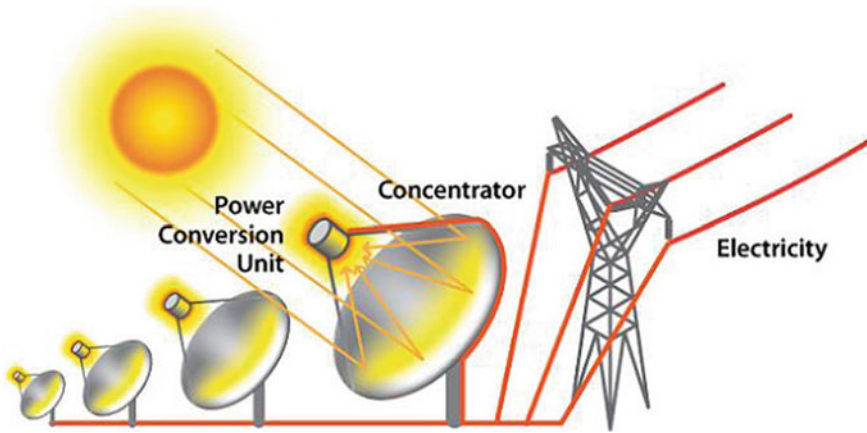**Fig. 12** Scheme of a solar tower concentrating system for electricity generation [21]

Fig. 13 Solar Dish/Engine power plant illustration [22]

heat storage for later use at night or on cloudy days. The idea behind using molten salt is its ability to store heat for a longer time than any other materials in a very efficient way. Due to the higher temperature associated with the solar tower system, it has higher efficiency, and better use of the energy storage system.

3. *Dish Engine Systems*

Figure 13 [22] shows a schematic for the dish engine system. The dish should track the sun motion to capture the maximum possible energy. The receiver is attached to a special combustion engine through tubes containing hydrogen or helium gas that can drive a special engine to generate mechanical power. The mechanical power generated from the engine is used to generate the electric power.

4. *Linear Fresnel Collectors (LFCs)*

LFCs utilizes a series of long flat, or slightly curved, mirrors positioned at various angles to focus sunlight on both sides of the fixed receiver [19]. A schematic for the linear Fresnel reflector power plant is shown in Fig. 14 [23].
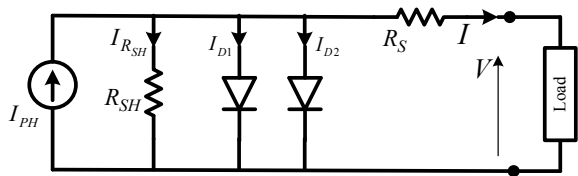
2 MPPT of PV Systems

Much research is developed to mathematically implement the PV-cell model. The two-diode model has been utilized in numerous literature [29–31] as appeared in Fig. 15 and Eq. (1).

$$I = I_{PH} - I_{sat1} * \left[e^{\left(\frac{q}{KT}(V+R_s I) \right)} - 1 \right] - I_{sat2} * \left[e^{\left(\frac{q}{2KT}(V+R_s I) \right)} - 1 \right] - \frac{V + R_s I}{R_{sh}}$$

$$(1)$$
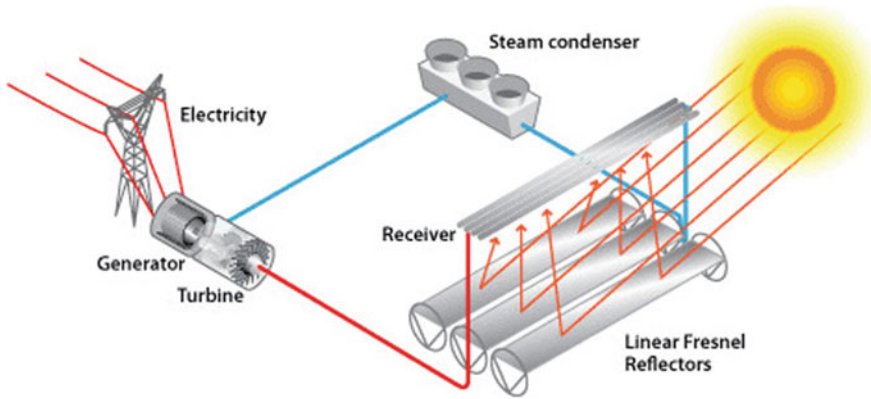
Fig. 14 A linear Fresnel reflector power plant [23]


Fig. 15 The two-diode
model

The model of one-diode is more extensively utilized than the model of two-diode for simulation due to its effortlessness with satisfactory exactness. Moreover, its parameter can be gotten tentatively with basic and exact procedures [32, 33]. Therefore this model will be utilized in this chapter. This model of PV-cell is appeared in Fig. 16 and Eq. (2).

$$I = I_{PH} - I_{sat1} * \left[e^{\left(\frac{q}{KT}(V + R_s I) \right)} - 1 \right] - \frac{V + R_s I}{R_{sh}} \tag{2}$$

MPPT needs a quick and intelligent controller to neutralize the rapid changes in weather and load. MPPT comprises the dc-dc converter and its controller as appeared in Fig. 17. Numerous approaches are acquainted with determining the MPP of PV systems as detailed in [29, 34–38].
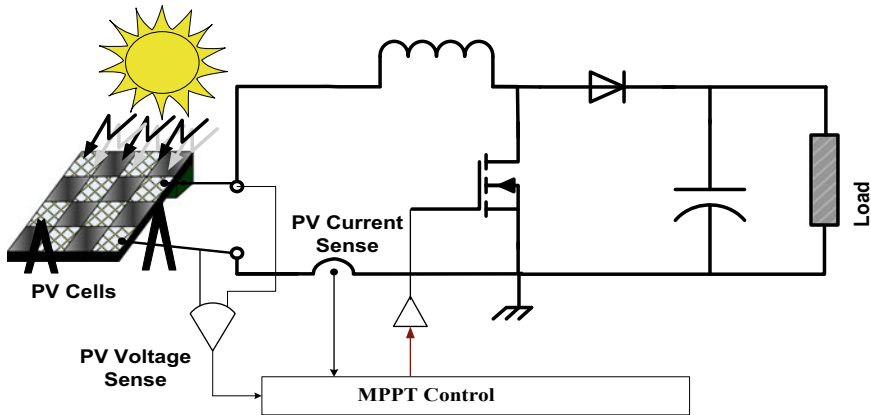

Fig. 16 The one-diode
model
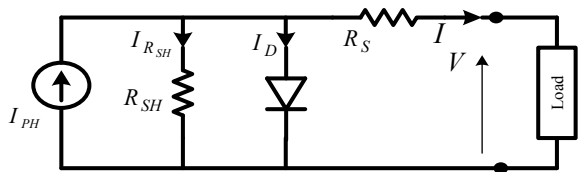
Fig. 17 The MPPT within the PV energy system [1]

1. *Constant Ratio Technique*

From the P-V curve, it is clear that the ratio of the maximum voltage of the array energy, V_{mp}, to the open-circuit voltage, V_{oc}, is approximately constant. Therefore, the PV array can be forced to act as a ratio of open-circuit voltage. The literature indicates a 73 to 80% achievement of V_{oc} [39]. Also, the relationship between the short circuit current and the current connection to the maximum power (MP) is almost constant. Therefore, it is possible to use the constant current MPPT algorithm that approximates the current MPP as a fixed ratio of short circuit current [40, 41]. The instantaneous infiltration of continuous voltage or current can be avoided by using a pilot cell [42].

2. *Perturb and Observe (P&O) Technique*

Perturb and observe (P&O) is one of the most popular techniques used in MPP tracking. This process is performed by periodically disrupting the system by increasing the array operation voltage and observing its effect on the output power of the array. Due to a fixed step-width, the system will experience high fluctuations, especially under unstable environmental conditions, resulting in loss of power in the PV system. This technique suffers from the wrong process, especially if multiple local maxima may occur in the case of partial shading [43, 44].

As appeared in Fig. 5 if the operating voltage of the PV module changes and the power increase the control system moves the point of operation of the PV module in that direction; otherwise the operating point is moved in the opposite direction. The flowchart appears in Fig. 18 and the simulation is included in the PSIM software package as appeared in Fig. 19. A common problem with this technique is that the final voltage of the PV unit is confused with each MPPT cycle. Therefore, when the MPP is reached, the output power oscillates around the maximum, which leads to power loss in the PV system. A modified P&O technique was introduced in [45] to solve this problem by multiplying the change in charge ratio (DR) by a dynamic constant
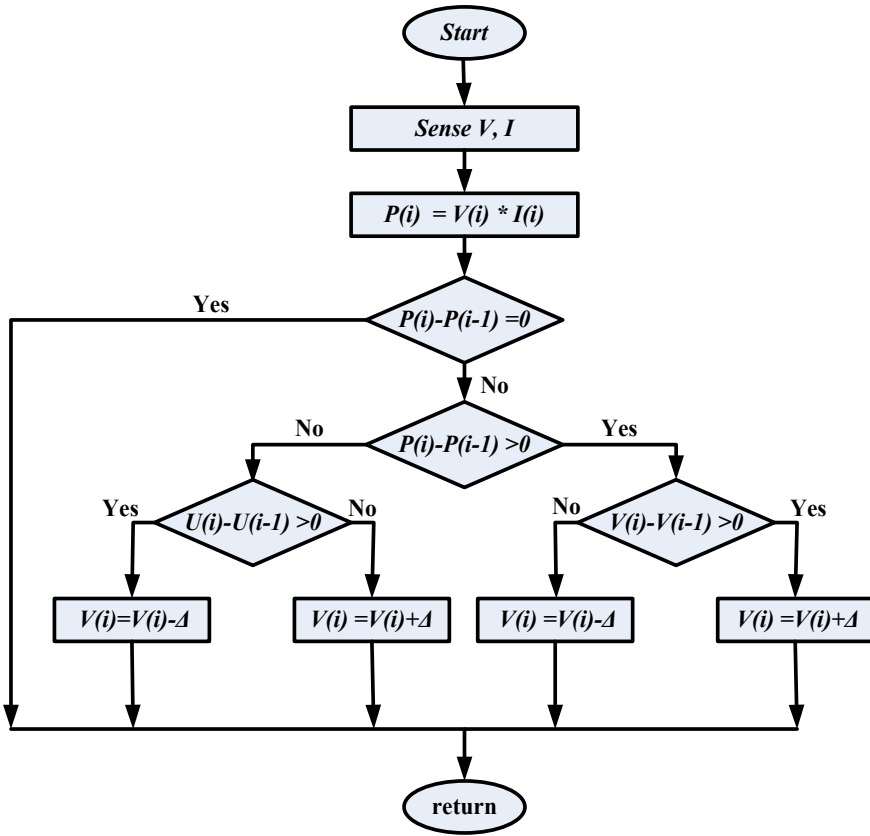
Fig. 18 State-flowchart of P&O MPPT

based on the previous change in the energy extracted as shown in Eq. (3). Another technique [46] ANN was used to predict this fixed multiplier. These technologies complicate the system and may lead to more fluctuations in stable weather conditions [29]. Several amendments were made to this technique in literature [47–49].

The adjusting factor for the change in DR of the modified P&O technique can be obtained from the following equation:

$$M = \frac{|\Delta D|}{|\Delta P|} \tag{3}$$

Where ΔP is the change of output power, ΔD is the change in DR.

3. *Incremental Conductance Technique (INC)*

Auxiliary conductivity technology is widely used due to its high tracking accuracy instability and being able to adapt well to rapidly changing weather conditions [50].
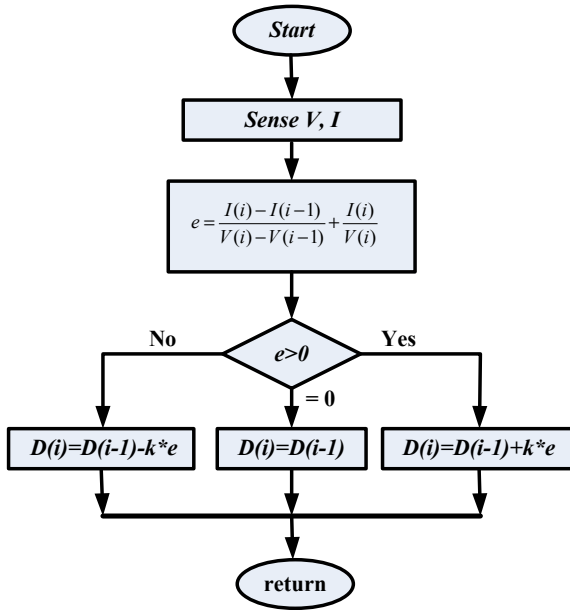
Fig. 19 P&O MPPT control with PSIM [13]

Incremental conductivity (IncCond) is based on a comparison of the instantaneous conductivity of the plate with the additional conductivity of the plate. The input impedance of the DC-DC adapter is matched with the optimum impedance of the PV board. The PV module derivative is given as in Eq. (4), the error equation (e) is the same as in Eq. (5) [51–53].

$$\frac{dP}{dV} = \frac{d(V \times I)}{dV} = I + V \frac{dI}{dV} = 0 \tag{4}$$

$$e = \frac{I(i) - I(i-1)}{V(i) - V(i-1)} + \frac{I(i)}{V(i)} \tag{5}$$

Therefore, MPP tracking requires the following procedure as shown in Fig. 20. It can be implemented by a simple integration unit with an error signal (e) which is the input and the scaling factor k. The function k is to adjust the error signal e to an appropriate range before the full compensator. Since the error signal e becomes smaller as the operating point approaches MPP. Therefore, smooth tracking and adaptation can be achieved [51].

A dynamic step-by-step change in volume was introduced for INC to effectively improve MPPT speed and accuracy simultaneously [50]. This technology improves the performance of INC technology but increases the complexity of the control

Fig. 20 State-flowchart of INC MPPT [13]

system. The INC flow chart is shown in Fig. 20 and simulation included in the PSIM software package as shown in Fig. 21.

4. *Hill Climbing Technique (HC)*

HC technique utilizes a boost converter duty cycle as the judging parameter [54, 55]. The flow diagram of the HC technique is shown in Fig. 22. This technique was incorporated and emulated into the PSIM software as appeared in Fig. 23.
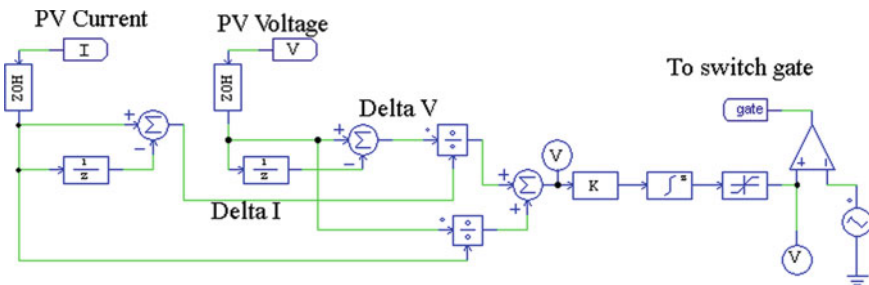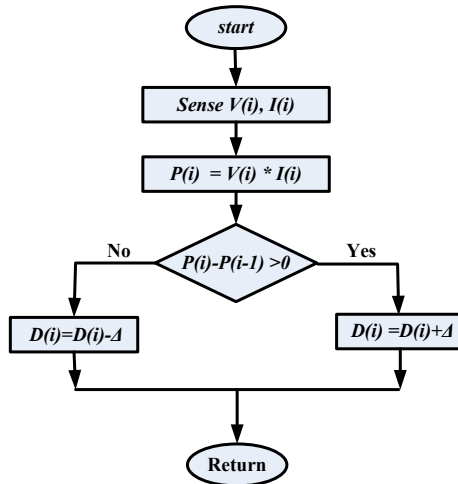

Fig. 21 INC MPPT control with PSIM [13]

Fig. 22 State-flowchart of HC-MPPT
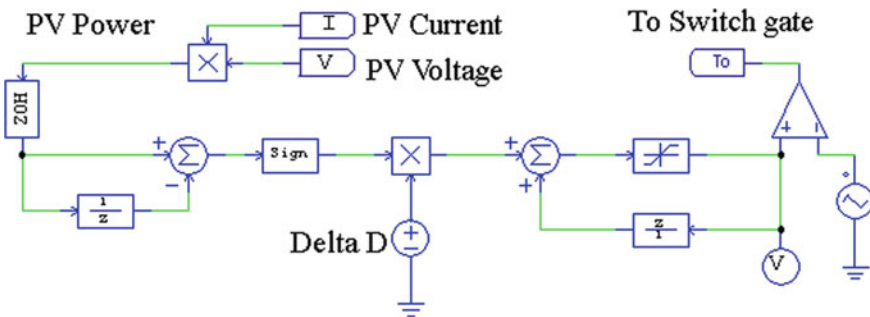
Fig. 23 HC-MPPT Control with PSIM

3 The Performance of MPPT of PV Systems Under Partial Shading Conditions

Partial shading occurs when one or more of the PV-cells in the PV array are introduced to different radiations [56–58]. When this happens, the photovoltaic cell shading will work with the current higher than the generated current and act as a load for the other photovoltaic cells. Due to the increased current flow in the shaded PV-cell higher than the generated current, the voltage ends in negative on this PV-cell as shown in Fig. 24 of PV-cells in the series with 500 and 1000 W/m². Figure 25 shows the relationship between the forces generated by two series of cells and the resulting PV voltage along with the shaded photocell radiation. The relationship between the shaded photoelectric cell forces of two PV series systems with a variety of their final potential with this cell radiation is shown in Fig. 26
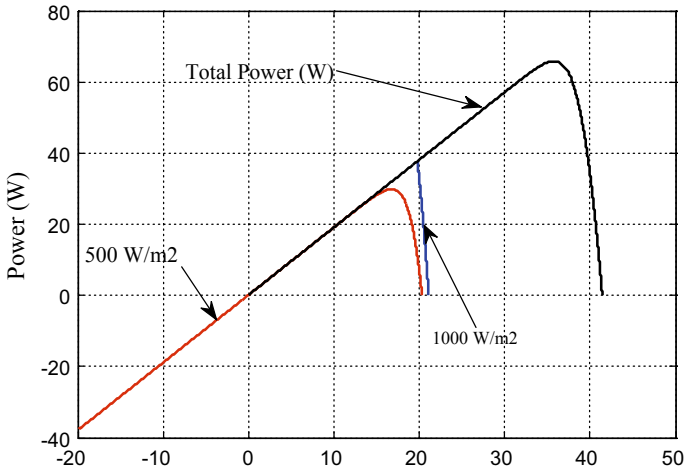
Fig. 24 PV-cell' terminal voltage of the two series PV-cells without bypass diode

**Fig. 25** The two P-V cells total power without bypass
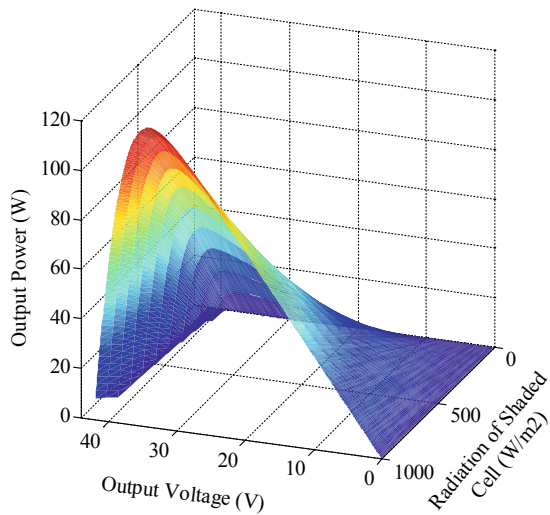
[59, 60]. Figure 27 demonstrates the variety-generated power of 20 series PV-cells with the terminal voltage and radiation on the shaded PV cell when other cells are exposed to 1000 W/m^2 radiation. Figure 28 demonstrates the power of shaded PV cell among 20 series PV-cells along with its terminal voltage and the radiation of these cells where the rest of PV-cells is 1000 W/m^2. It is clear from the above discourse that, the hotspot can be increasingly risky for a higher number of series PV cells. A few kinds of literature work in the optimum number of PV-cells on series to prevent its damage due to the hotspot [59, 60].

**Fig. 26** The shaded cell power with its voltage and radiation
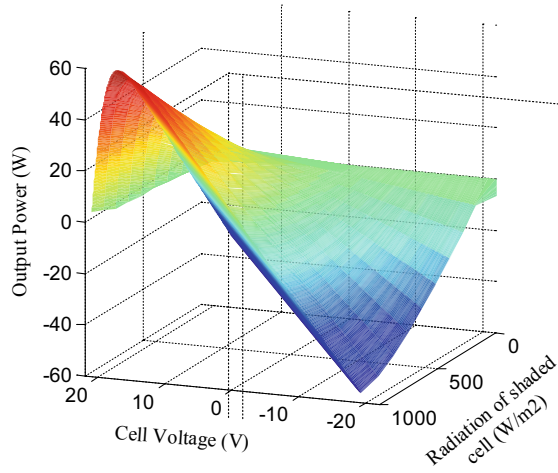
**Fig. 27** Total power of 20 series with one shaded PV-cells
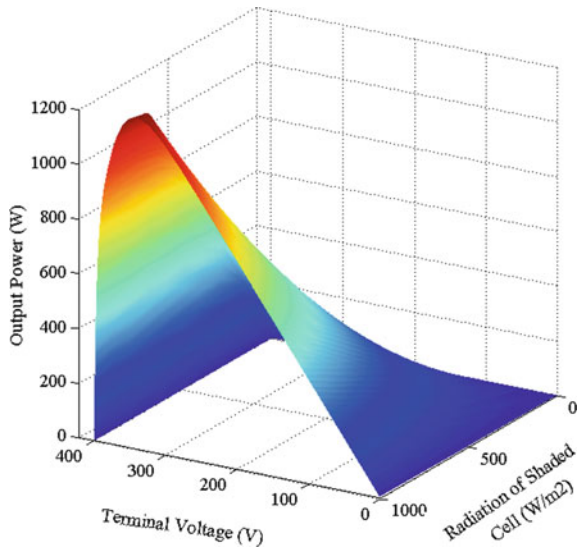
A wide range of literature has been produced to treat the influence of PV hotspots [61, 62]. One of the best ways is to include the side diode next to each PV-cell or it can be associated with a certain number of photovoltaics to reduce the cost of photovoltaics and reduce the losses of the PV system. In the case of two series of photovoltaic cells with bypass diodes, the relationship between the terminal voltage and the output energy of these two photovoltaic cells with radiation of 1000 and 500 W/m^2 is shown in Fig. 29. Figure 30 shows the relationship between the output

Fig. 28 The power of shaded PV-cell among 20 series PV-cells
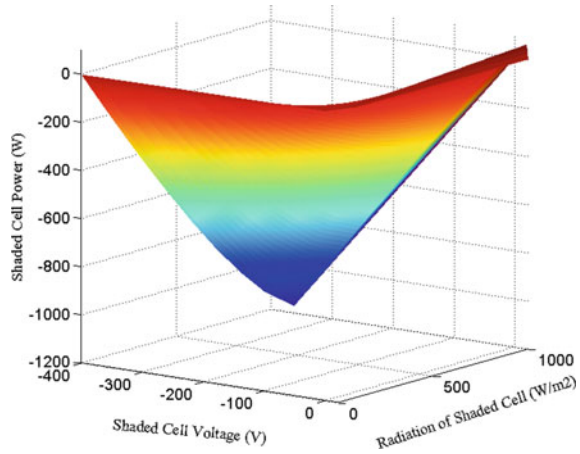
Fig. 29 The output power and terminal voltage relation for two series PV-cells with bypass diodes
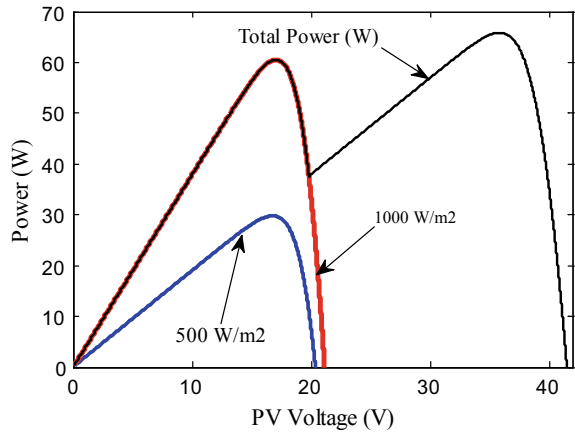

energy and the terminal voltage of two series of bypass photovoltaic cells in a different shading state when the radiation of the other photovoltaic cells is 1000 W/m².

In the case of 20 series of diode-connected photovoltaic cells connected to each of them, the total form of the energy generated by the different radiation of the shaded photovoltaic cells is shown in Fig. 31 The rest of the radiation in other PV-cells is 1000 W/m². It is clear from this figure that the shaded PV-cell begins to operate when the terminal voltage forces the shaded PV-cell voltage to be positive. Figure 32 shows the relationship between the energy output of shaded photovoltaic cells and their voltage for multiple radiations for this cell.

There are three MPP showed up in Fig. 33, the global peak (GP) is the one relating to point#2. The MPPT system ought to pursue the global MPP which is #2 as appeared in Fig. 33.

Fig. 30 The output power and terminal voltage relation for two series PV-cells with bypass diodes under various irradiances
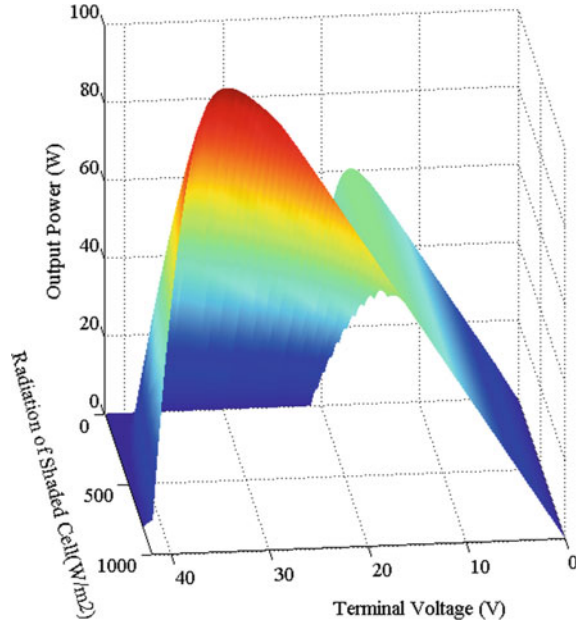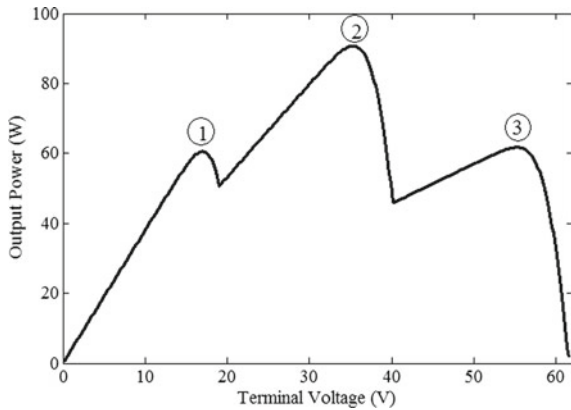

Fig. 31 The total generated power along with terminal voltage for different radiation of shaded PV-cell in case of 20 series PV-cells with bypass diodes
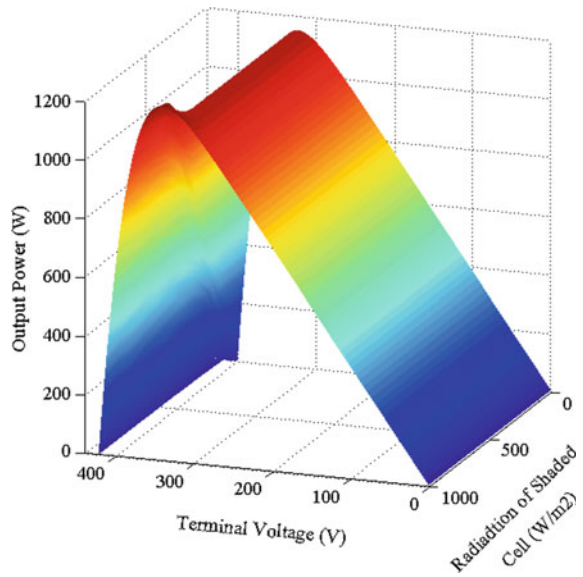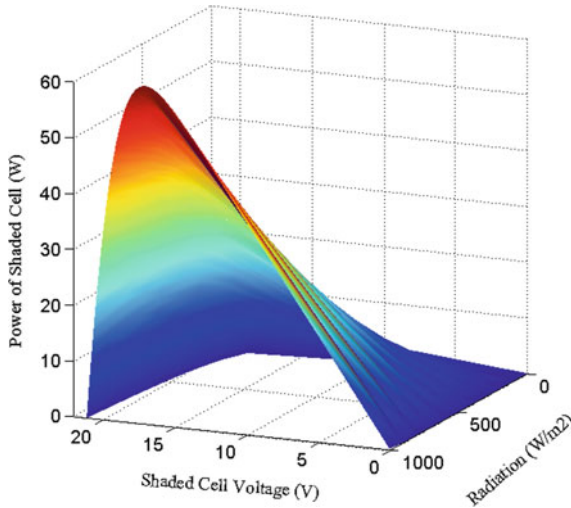
Fig. 32 The relation between the output power of shaded PV-cell and its voltage for different radiation of this cell

Fig. 33 The relation between the generated power and terminal voltage in case of three series PV-cells at radiation of 1000, 700, 300 W/m^2

A. Mismatch Power Loss

The relationship between the peak strength and the sum of the peaks is called a mismatch loss (MML) and can be calculated mathematically as shown in Eq. (6). Along these lines, the more MML, the more energy is generated from the photoelectric system and vice versa. If the entire photovoltaic cells had the same radiation and the entire photovoltaic system worked in the MPP and each cell operated in its MPP, then the MML factor would be 100%. The value of the MML factor can be obtained from the accompanying equation:

$$MML = \frac{\text{Maximum power of whole PV system}}{\sum\limits_{i=1}^{N} P\text{max}(i)} * 100 \qquad (6)$$

where N is the total number of PV-cells in the PV system.

B. Fuzzy Controller MPPT Technique

Initially, the Fuzzy Logic Control (FLC) has been in focus since 1920 [63]. By 1965 another exploration [64] had introduced FLC as a console for real applications. Since that time FLC has been applied to many applications in various fields of science [65]. FLC can be effectively implemented in various digital devices, for example, microcontrollers [43, 66] digital signal processors, DSP [67] and field-programmable gate group, FPGA, [43, 68] and end up developing Innovation in industrial applications. One of the valuable uses for FLC is the MPPT for PV systems.

C. PSO MPPT Technique

PSO is one of Swarm Intelligence techniques that use randomized population-based variables to solve optimization problems. This technology was first introduced by Eberhart and Kennedy (1995) [69]. The first PSO work was used in MPPT from PV systems implemented in 2004 [70]. PSO is inspired by the behavior of social swarm from school education or bird rising. An evolutionary PSO process, potential solutions, called particles; move around the multidimensional search space by following and tracking the best current particle position in a swarm. The PSO process can be illustrated in the following [71]:

Every particle in the swarm has two variables: position vector $x_i(t)$ and velocity vector $v_i(t)$ as appeared in Eq. (7). Therefore, every particle $x_i(t)$ is described by a vector $[x_{i1}(t), x_{i2}(t),\ldots,x_{iD}(t)]$, as i is the index number of every particle, D is the dimension of the search space and t is iteration number.

$$x_i(t + 1) = x_i(t) + v_i(t + 1) \qquad (7)$$

$x_i(t)$, $v_i(t)$, and the global best position $G_i(t)$ are utilized to set the new position of the particle by calculating the velocity as follows:

$$v_i(t + 1) = \underbrace{\omega(t)v(t)}_{\text{Inertial parameters}} + \underbrace{c_1 r_1 (P_i(t) - x_i(t))}_{\text{Personal best velocity components}} + \underbrace{c_2 r_2 (G_i(t) - x_i(t))}_{\text{Global best velocity component}} \qquad (8)$$

where, $\omega(t)$ is the inertia weight factor that controls the search space exploration. The value of $\omega(t)$ can be chosen as a constant value equal to 0.5 or as a variable value for the obtained *GP* acceleration [72]. c_1 and c_2 are acceleration constants, which provide weight to individual and social *GP* components, individually. Where c1 is self-confidence; Range: 1.5–2; and c_2 is swarm confidence. Range: 2–2.5 [73].

A modified PSO technology named deterministic PSO (DPSO) [74] was used to improve MPPT performance under a partial shading component. Also, hill climbing (HC-MPPT) has been used in the uniform distribution of insolation on the PV system but DPSO will be used in the case of PSC. The authors used three parallel branches and four PV units in the series [74]. Another research [75] has suggested a great idea to use some particles to locate the LP and some other particles to find a global peak (GP).

A modified PSO (MPSO) technique [76] was used to adjust the weight of inertia, using the principles of a genetic algorithm (GA) to improve its strength while searching for a GP. The adjusted inertial weight ω can be obtained from the Eq. (9) which uses the main GA principles by increasing the inertial weight value ω at the beginning (in the global research phase) and reducing it to a precise increase at the end of the improvement when the particles approach the optimal solution.

$$\omega(k) = \omega_s - (\omega_s - \omega_e)(T_m - k)/T_m \tag{9}$$

where$_s$ is the initial inertia weight, ω_e is the inertia weight when reaching maximum inertia times, and T_m is the maximum inertia times.

D. Simulation of Proposed Systems

A simulation model of three PV units and a boost transformer used in FLC and MPSO is shown in Fig. 34. The simulation model for the system proposed in SIMULINK is shown in Fig. 35. The simulation parameters for the PV unit are shown in Table 1.

The results of MPSO and FLC simulation are shown in Fig. 36. The response of different MPPT techniques is evaluated in rapidly changing weather conditions. The simulation time shown in this figure is divided into six periods of about two seconds each. Every two seconds, the radiation will be changed in two PV units out of three and the first will be stationary (1000 W/m2) throughout the simulation time (Fig. 37).
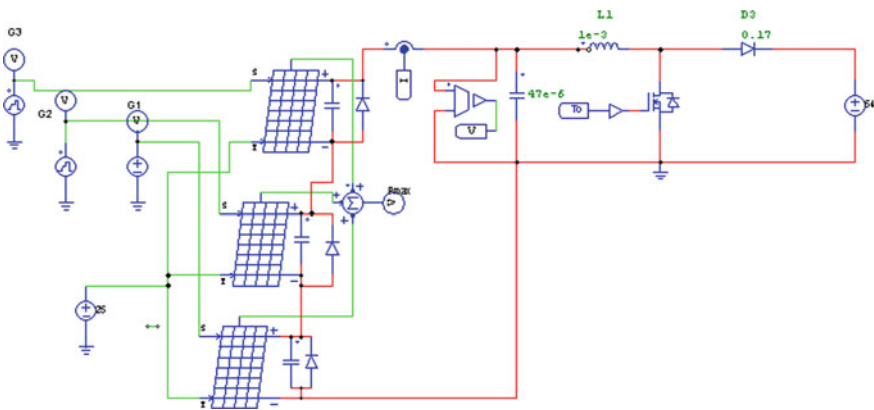
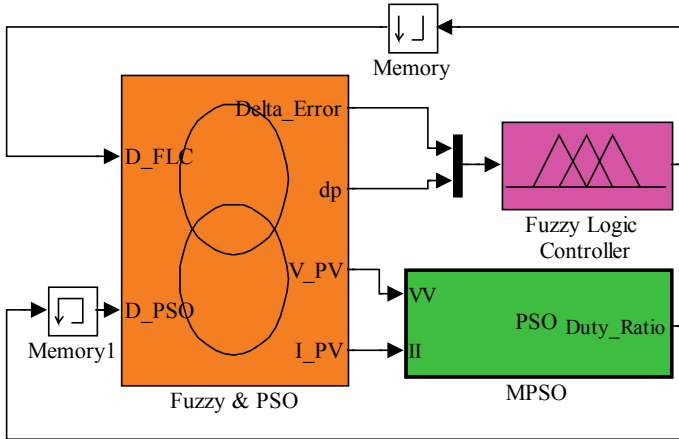**Fig. 34** The simulation model for PV modules and boost converter

Fig. 35 The SIMULINK model showing the co-simulation between SIMULINK and PSIM

Table 1 Simulation parameters of each PV Module in PSIM [54]

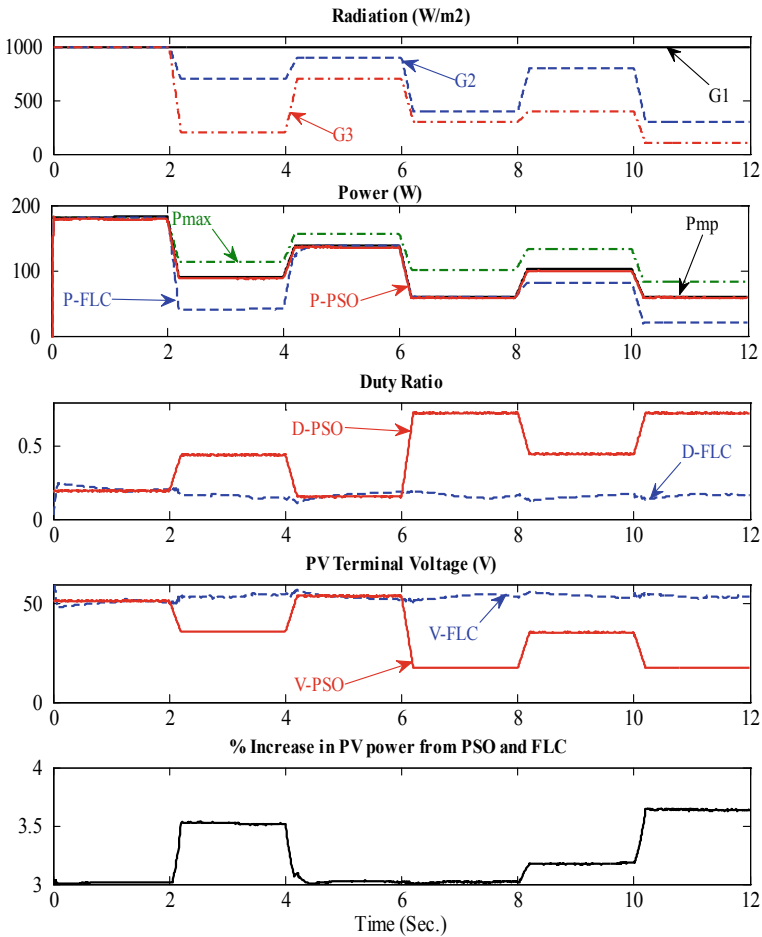**Fig. 36** The simulation results of MPSO and FLC

4 Conclusion

In this chapter, various techniques for tracking, analyzing, simulating, and comparing maximum power points are demonstrated. MATLAB/SIMULINK/PSIM is used to model the photoelectric system under partial shading conditions. Moreover, the response of various power point tracking techniques in rapidly changing weather conditions is evaluated.
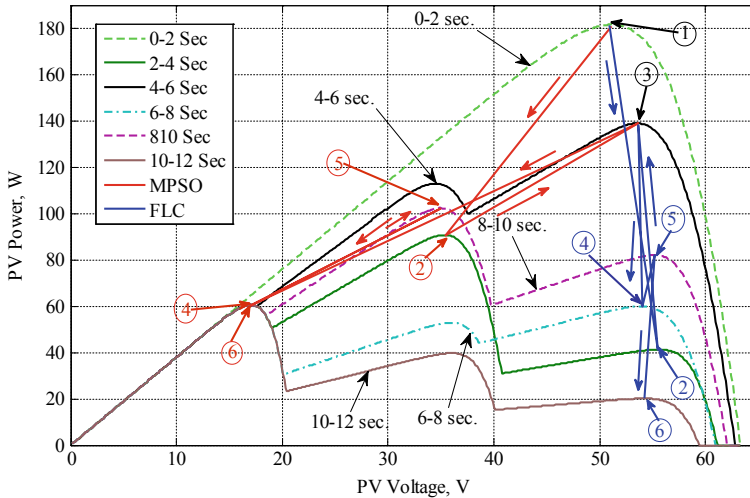
Fig. 37 The relation between the generated power along with terminal voltage and the MPPT response for MPSO and FLC

References

1. Eltamaly AM, Al-Saud MS, Abokhalil AG, Farh HMH (2020) "Simulation and experimental validation of fast adaptive particle swarm optimization strategy for photovoltaic global peak tracker under dynamic partial shading. Renew Sustain Energy Rev 124:109719

2. Eltamaly AM, Al-Saud MS, Abokhalil AG (2020) A novel bat algorithm strategy for maximum power point tracker of photovoltaic energy systems under dynamic partial shading. IEEE Access 8:10048–10060

3. Eltamaly AM, Farh HMH (2020) PV Characteristics, Performance and Modelling. In: Modern maximum power point tracking techniques for photovoltaic energy systems. Springer, Cham, pp 31–63

4. Gong X, Dong F, Mohamed MA, Awwad EM, Abdullah HM, Ali ZM (2020) Towards distributed based energy transaction in a clean smart island. J Clea Prod 122768

5. Eltamaly AM, Farh HMH, Al Saud MS (2019) Impact of PSO reinitialization on the accuracy of dynamic global maximum power detection of variant partially shaded PV systems. Sustainability 11(7):2091

6. Lee TD, Ebong AU (2017) A review of thin film solar cell technologies and challenges. Renew Sustain Energy Rev 70:1286–1297

7. Adib R, Murdock HE, Appavou F, Brown A, Epp B, Leidreiter A, Lins C et al (2015) Renewables 2015 global status report. REN21 Secretariat, Paris, France

8. Eltamaly AM, Mohamed MA (2018) Optimal sizing and designing of hybrid renewable energy systems in smart grid applications. In: Advances in renewable energies and power technologies. Elsevier, pp 231–313

9. Mohamed MA, Eltamaly AM (2018) A novel smart grid application for optimal sizing of hybrid renewable energy systems. In: Modeling and simulation of smart grid integrated with hybrid renewable energy systems. Springer, Cham, pp 39–51

10. Eltamaly AM, Mohamed MA, Alolah AI (2016) A novel smart grid theory for optimal sizing of hybrid renewable energy systems. Sol Energy 124:26–38

11. A Review of Concentrated Solar Power in 2014. https://www.engineering.com/ElectronicsDesign/ElectronicsDesignArticles/ArticleID/9286/A-Review-of-Concentrated-Solar-Power-in-2014.aspx

12. Motahhir S, Chouder A, El Hammoumi A, Benyoucef AS, El Ghzizal A, Kichou S, Kamel K, Sanjeevikumar P, Silvestre S (2020) Optimal energy harvesting from a multistrings PV generator based on artificial bee colony algorithm. IEEE Syst J

13. Rezk H, Eltamaly AM (2015) A comprehensive comparison of different MPPT techniques for photovoltaic systems. Sol Energy 112:1–11

14. Eltamaly AM (2015) Performance of smart maximum power point tracker under partial shading conditions of photovoltaic systems. In: J Renew Sustain Energy 7(4): 043141

15. Kroposki B, Margolis R, Ton D (2009) Harnessing the sun. IEEE Power Energ Mag 7(3):22–33

16. Eltamaly AM (2018) Performance of MPPT techniques of photovoltaic systems under normal and partial shading conditions. In: Advances in renewable energies and power technologies. Elsevier

17. Mohamed MA, Eltamaly AM, Alolah AI (2017) Swarm intelligence-based optimization of grid-dependent hybrid renewable energy systems. Renew Sustain Energy Rev 77:515–524

18. Mohamed MA, Eltamaly AM, Alolah AI (2016) PSO-based smart grid application for sizing and optimization of hybrid renewable energy systems. PLoS ONE 11(8):e0159702

19. Eltamaly AM, Al-Shamma'a AA (2016) Optimal configuration for isolated hybrid renewable energy systems. J Renew Sustain Energy 8(4):045502

20. Mohamed MA, Eltamaly AM (2018) Modeling and simulation of smart grid integrated with hybrid renewable energy systems. Springer, New York

21. Eltamaly AM, Mohamed MA, Al-Saud MS, Alolah AI (2017) Load management as a smart grid concept for sizing and designing of hybrid renewable energy systems. Eng Optimi 49(10):1813–1828

22. Mohamed MA, Eltamaly AM, Alolah AI (2015) Sizing and techno-economic analysis of stand-alone hybrid photovoltaic/wind/diesel/battery power generation systems. J Renew Sustain Energy 7(6):063128

23. Eltamaly AM (2015) Performance of smart maximum power point tracker under partial shading conditions of PV systems. In: 2015 IEEE International Conference on Smart Energy Grid Engineering (SEGE). IEEE, pp 1–8

24. Al-Saud M, Eltamaly AM, Mohamed MA, Kavousi Fard A (2019) An intelligent data-driven model to secure intra-vehicle communications based on machine learning. IEEE Trans Ind Electr

25. Eltamaly AM, Farh HMH (2019) Dynamic global maximum power point tracking of the PV systems under variant partial shading using hybrid GWO-FLC. Solar Energy 177: 306–316

26. Mohamed MA, Eltamaly AM, Farh HM, Alolah AI (2015) Energy management and renewable energy integration in smart grid system. In: 2015 IEEE international conference on smart energy grid engineering (SEGE). IEEE, pp 1–6

27. Eltamaly AM, Addoweesh KE, Bawa U, Mohamed MA (2014) Economic modeling of hybrid renewable energy system: a case study in Saudi Arabia. Arab J Sci Eng 39(5):3827–3839

28. Farh HMH, Othman MF, Eltamaly AM, Al-Saud MS (2018) Maximum power extraction from a partially shaded PV system using an interleaved boost converter. Energies 11(10):2543

29. Eltamaly AM, Farh HMH, Othman MF (2018) A novel evaluation index for the photovoltaic maximum power point tracker techniques. Solar Energy 174:940–956

30. Farh HMH, Eltamaly AM, Othman MF (2018) Hybrid PSO-FLC for dynamic global peak extraction of the partially shaded photovoltaic system. PloS one 13(11):e0206171

31. Eltamaly AM, Farh HMH, Al-Saud MS (2019) Grade point average assessment for meta-heuristic GMPP techniques of partial shaded PV systems. IET Renew Power Gener 13(8):1215–1231

32. Farh HMH, Othman MF, Eltamaly AM (2017) Maximum power extraction from grid-connected PV system. In 2017 Saudi Arabia Smart Grid (SASG). IEEE, pp 1–6

33. Farh HMH, Eltamaly AM, Al-Saud MS (2019) Interleaved boost converter for global maximum power extraction from the photovoltaic system under partial shading. IET Renew Power Gener 13(8):1232–1238

34. Motahhir S, Hammoumi AEL, Ghzizal AEL, Derouich A (2019) Open hardware/software test bench for solar tracker with virtual instrumentation. Sustain Energy Technol Assess 31: 9–16

35. Etamaly AM, Mohamed MA, Alolah AI (2015) A smart technique for optimization and simulation of hybrid photovoltaic/wind/diesel/battery energy systems. In: 2015 IEEE International conference on smart energy grid engineering (SEGE). IEEE, pp 1–6

36. Eltamaly AM, Al-Saud MS, Abo-Khalil AG (2020) Performance improvement of pv systems' maximum power point tracker based on a scanning PSO particle strategy. Sustainability 12(3):1185

37. Balouktsis A, Karapantsios TD, Anastasiou K, Antoniadis A, Balouktsis I (2006) Load matching in a direct-coupled photovoltaic system-application to Thevenin's equivalent loads. Int J Photoenergy

38. Eltamaly AM, El-Tamaly HH, Enjeti P (2002) An improved maximum power point tracker for photovoltaic energy systems. In: The 2nd Minia international conference for advanced trends in engineering

39. Eltamaly AM, Al-Saud MS, Abokhalil AG (2020) A novel scanning bat algorithm strategy for maximum power point tracker of partially shaded photovoltaic energy systems. Ain Shams Eng J

40. Eltamaly AM, Al-Saud MS, Abokhalil AG, Farh HMH (2020) Photovoltaic maximum power point tracking under dynamic partial shading changes by novel adaptive particle swarm optimization strategy. Trans Inst Measurement Control 42(1):104–115

41. Yuvarajan S, Xu S (2003) Photo-voltaic power converter with a simple maximum-power-point-tracker. In: Proceedings of the 2003 international symposium on circuits and systems, vol 3. ISCAS'03. IEEE, pp III–III

42. Veerachary M, Senjyu T, Uezato K (2002) Voltage-based maximum power point tracking control of PV system. IEEE Trans Aerosp Electron Syst 38(1):262–270

43. Eltamaly AM, Alolah AI, Abdulghany MY (2010) Digital implementation of general purpose fuzzy logic controller for photovoltaic maximum power point tracker. In: SPEEDAM 2010. IEEE, pp 622–627

44. Farh HMH, Eltamaly AM (2020) Maximum power extraction from the photovoltaic system under partial shading conditions. In: Modern maximum power point tracking techniques for photovoltaic energy systems. Springer, Cham, pp 107–129

45. Al-Diab A, Sourkounis C (2010) Variable step size P&O MPPT algorithm for PV systems. In: 2010 12th International conference on optimization of electrical and electronic equipment. IEEE, pp 1097–1102

46. Mohamed MA, Eltamaly AM (2018) Sizing and techno-economic analysis of stand-alone hybrid photovoltaic/wind/diesel/battery energy systems. In: Modeling and simulation of smart grid integrated with hybrid renewable energy systems. Springer, Cham, pp 23–38

47. Femia N, Granozio D, Petrone G, Spagnuolo G, Vitelli M (2007) Predictive & adaptive MPPT perturb and observe method. IEEE Trans Aerosp Electron Syst 43(3):934–950

48. Eltamaly AM, Mohamed MA (2016) A novel software for design and optimization of hybrid power systems. J Braz Soc Mech Sci Eng 38(4):1299–1315

49. El-Tamaly HH, El-Tamaly AM, El-Baset Mohammed AA (2003) Design and control strategy of utility interfaced PV/WTG hybrid system. In: The ninth international middle east power system conference. MEPCON, pp 16–18

50. Liu F, Duan S, Liu F, Liu B, Kang Y (2008) A variable step size INC MPPT method for PV systems. IEEE Trans Industr Electron 55(7):2622–2628

51. Abouobaida H, Cherkaoui M (2012) Comparative study of maximum power point trackers for fast changing environmental conditions. In: 2012 International conference on multimedia computing and systems. IEEE, pp 1131–1136

52. Eltamaly AM, Mohamed MA (2014) A novel design and optimization software for autonomous PV/wind/battery hybrid power systems. Math Probl Eng

53. Siri K, Conner KA (2001) Fault-tolerant scaleable solar power bus architectures with maximum power tracking. In: APEC 2001. Sixteenth annual IEEE applied power electronics conference and exposition (Cat. No. 01CH37181), vol 2. IEEE, pp 1009–1014
54. Farh HMH, Eltamaly AM, Ibrahim AB, Othman MF, Al-Saud MS (2019) Dynamic global power extraction from partially shaded photovoltaic using deep recurrent neural network and improved PSO techniques. Int Trans Electr Energy Syst 29(9): e12061
55. Eltamaly AM, Addoweesh KE, Bawah U, Mohamed MA (2013) New software for hybrid renewable energy assessment for ten locations in Saudi Arabia. J Renew Sustain Energy 5(3):033126
56. Rajesh R, Carolin Mabel M (2014) Efficiency analysis of a multi-fuzzy logic controller for the determination of operating points in a PV system. Solar Energy 99:77–87
57. Kimball JW, Krein PT (2007) Digital ripple correlation control for photovoltaic applications. In: 2007 IEEE power electronics specialists conference. IEEE, pp 1690–1694
58. Mohamed MA, Eltamaly Am (2018) Introduction and literature review. In: Modeling and simulation of smart grid integrated with hybrid renewable energy systems. Springer, Cham, pp 1–10
59. Rossi D, Omaña M, Giaffreda D, Metra C (2014) Modeling and detection of hotspot in shaded photovoltaic cells. IEEE Trans Very Large Scale Integr (VLSI) Syst 23(6):1031–1039
60. Solórzano J, Egido MA (2014) Hot-spot mitigation in PV arrays with distributed MPPT (DMPPT). Sol Energy 101:131–137
61. Eltamaly AM, Abdelaziz AY eds (2019) Modern maximum power point tracking techniques for photovoltaic energy systems. Springer
62. Kim K (2014) Hot spot detection and protection methods for photovoltaic systems. PhD diss., University of Illinois at Urbana-Champaign
63. Libkin L (2016) SQL's three-valued logic and certain answers. ACM Trans Database Syst (TODS) 41(1):1–28
64. Mendel JM (2007) Type-2 fuzzy sets and systems: an overview. IEEE Comput Intell Mag 2(1):20–29
65. Eltamaly Am (2010) Modeling of fuzzy logic controller for photovoltaic maximum power point tracker. In: Solar Future 2010 Conference, Istanbul, Turkey
66. Boukens M, Boukabou A (2013) PD with fuzzy compensator control of robot manipulators: Experimental study. In: 3rd International conference on systems and control. IEEE, pp 973–978
67. Eltamaly AM (2011) Modeling of fuzzy logic controller for photovoltaic maximum power point tracker. Trends Electr Eng 1(2)
68. Tipsuwanpom R, Runghimmawan T, Intajag S, Krongratana V (2004) Fuzzy logic PID controller based on FPGA for process control. In: 2004 IEEE international symposium on industrial electronics, vol 2. IEEE, pp 1495–1500
69. Farh HM, Eltamaly AM, Mohamed MA (2012). Wind energy assessment for five locations in Saudi Arabia. In: International conference on future environment and energy (ICFEE 2012,) IPCBEE (2012) © (2012) IACSIT Press, February 26–28. Singapoore
70. Mohamed MA, Eltamaly AM, Alolah AI, Hatata AY (2019). A novel framework-based cuckoo search algorithm for sizing and optimization of grid-independent hybrid renewable energy systems. Int J Green Energy 16(1):86–100
71. Eltamaly AM, Farh HMH, Abokhalil AG (2020). A novel PSO strategy for improving dynamic change partial shading photovoltaic maximum power point tracker. Energy Sour Part A Recovery, Utilization, Environ Effects, 1–15
72. Mohamed MA, Eltamaly AM (2018) A PSO-based smart grid application for optimum sizing of hybrid renewable energy systems. In: Modeling and simulation of smart grid integrated with hybrid renewable energy systems. Springer, Cham, pp 53–60
73. Ishaque K, Salam Z, Shamsudin A, Amjad M (2012) A direct control based maximum power point tracking method for photovoltaic system under partial shading conditions using particle swarm optimization algorithm. Appl Energy 99:414–422

74. Fu Q, Tong N (2010) A new PSO algorithm based on adaptive grouping for photovoltaic MPP prediction. In: 2010 2nd International workshop on intelligent systems and applications. IEEE, pp 1–5
75. Mohamed MA, Eltamaly AM (2018) Modeling of hybrid renewable energy system. In: Modeling and simulation of smart grid integrated with hybrid renewable energy systems. Springer, Cham, pp 11–21
76. PSIM (2020) Psim User Manual of PSIM computer Simulation. Accessed June 2020. http://powersimtech.com/wp-content/uploads/2015/05/PSIM-User-Manual.pdf